Adv Biochem Engin/Biotechnol (2005) 95: 107–142
DOI 10.1007/b102212
© Springer-Verlag Berlin Heidelberg 2005

Fluorescence Correlation Spectroscopy with Autofluorescent Proteins

Tobias Kohl[1] · Petra Schwille[2] (✉)

[1] Pastor-Sander-Bogen 92, 37083 Göttingen, Germany
tkohl1@web.de
[2] Institute of Biophysics, BioTec, TU Dresden; c/o Max-Planck-Institute for Molecular Cell Biology and Genetics, Pfotenhauerstrasse 108, 01307 Dresden, Germany
schwille@mpi-cbg.de

Abstract Fluorescence correlation spectroscopy (FCS) is a versatile technique operating at the single-molecule level, that successfully meets many challenges of modern biological research. Based on the detection of mobile fluorescent molecules diffusing in and out of a diffraction-limited laser focus, the method allows to resolve particle dynamics within cells and their compartments. Previous FCS studies have described various parameters of protein function, namely mobility, transport and localization phenomena, enzymatic turnovers of biochemical substrates and molecular association and dissociation reactions. Recent progress in the application of FCS to intracellular systems has particularly taken advantage of detecting autofluorescent proteins and their genetically encoded fusions to cellular proteins. This review discusses recent applications of FCS analysis with and on fluorescent proteins, particularly highlighting chemical and physical properties. Inherent limitations of the presented approaches are discussed in detail and strategies for optimisation of experimental systems outlined.

Keywords FCS · GFP · DsRed · Cross-correlation analysis · Single molecule · In vivo · Two-photon excitation · FRET · Blinking · Fluorescence resonance energy transfer

List of Abbreviations

FCS Fluorescence correlation spectroscopy
FRET Fluorescence resonance energy transfer
RFP Red fluorescent protein
TPE Two-photon excitation

1 Introduction

Biological research in the post-genomic era has so far been particularly concerned with predicting and studying protein function. To this end, experiments are increasingly performed in the live cell environment, taking advantage of fluorescence-based microscopic techniques that allow for real-time data acquisition, instead of employing cell extracts or purified recombinant proteins in biochemical assays. These in vivo methods rely on fluorescent reporter systems consisting of the protein of interest labelled with a fluorescent dye molecule. To minimize any interference with the cellular system, this is ideally realized by a genetic fusion with fluorescent proteins, so-called genetically encoded probes.

The present article focuses on a particular optical technique with single-molecule sensitivity, namely Fluorescence Correlation Spectroscopy (FCS) [1, 2], with a specific emphasis on its suitability for intracellular analysis of fluorescent proteins. FCS analyses minute spontaneous fluctuations in the fluorescence emission of small molecular ensembles to study underlying inter- and intramolecular dynamics. Combining single molecule sensitivity with large statistical averaging, fluctuation autocorrelation analysis allows for a highly quantitative simultaneous analysis of multiple molecular parameters, namely particle concentration and mobility, intramolecular dynamics and binding reactions. In addition to single-colour applications by autocorrelation analysis, dual-colour cross-correlation analysis has been established and proved particularly beneficial for the study of molecular association and dissociation events [3]. Since FCS observes fluorescent molecules at nanomolar or even lower concentrations, it is well suited to collect quantitative data under physiological conditions and monitor dynamic equilibria in vivo [4]. While bulk studies are typically performed at fairly high particle concentrations, subtle regulatory processes or cellular background activities might only be resolved at the single molecule level. Moreover, fluorescence correlation spectroscopy can be combined with two-photon excitation (TPE) conferring further advantages, in particular excitation of two or more spectrally different dyes with one laser line, and reducing cell damage and sample consumption by photobleaching [5–7]. Due to its sensitivity, FCS resolves intramolecular photodynamic processes of fluorescent proteins, like pH-dependent blinking [8–11].

Nevertheless, just like any other fluorescence-based technique, FCS benefits from the continued efforts for discovery and redesign of optimised fluorescent probes [12, 13]. Along with reporting recent applications of intracellular FCS [14–17] this article thus aims to provide a summary on fluorescent proteins (for thorough discussion see Miyawaki in this issue) from the specific viewpoint of their applicability in FCS experiments, with respect to their beneficial and limiting properties.

2
Theoretical and Practical Concepts of FCS

At first a brief introduction to the technique of Fluorescence Correlation Spectroscopy (FCS) shall be given, to lay the grounds for the discussion of applications following later in this review. Its large potential for simultaneous examination of molecular parameters like particle concentration, mobility, rate constants of intramolecular dynamics and molecular interactions has contributed to the present popularity and wide-spread application of FCS. Thus, the interested reader can be referred to a number of recent reviews and articles covering FCS in much more detail, addressing theoretical framework, technical setups, reported applications and practical aspects [18–21].

2.1 Autocorrelation Analysis

FCS is based on the universal formalism of correlation analysis, comparing time signals for series of lag times τ. In the common case, the signal results from fluorescence excitation and detection within a confocal volume [22]. The normalized fluorescence autocorrelation function is generally defined by

$$G(\tau) = \langle \delta F(t)\ \delta F(t+\tau)\rangle / \langle F(t)\rangle^2 \quad (1)$$

where $\delta F(t) \equiv F(t) - \langle F(t)\rangle$ describes the time-dependent fluctuation of fluorescence signals from a volume element $V_{eff} = \pi^{3/2}\omega_0^2 z_0$ (2). V_{eff} constitutes the detection volume (with ω_0 and z_0 describing the lateral and axial radius) that largely overlaps with the laser focus (Scheme 1). Fluorescence fluctuations principally result from fluorescing particles diffusing into and out of V_{eff} with a typical diffusion coefficient D_i (Scheme 1). The resulting fluctuation decay time τ describes the average particle residence time τ_{diff} within V_{eff}. Fluctuation amplitudes and their duration and temporal frequency of occurrence, are characteristic for the particle number within V_{eff}, the mode of particle movement and the presence of fast photodynamic processes. These contributions are represented in G(τ) by the particle number 'N', the characteristic diffusion behaviour '$G_M(\tau)$' and an additional factor induced by fast intra-molecular photodynamic processes. Scheme 1 presents the basic fitting models for autocorrelation curves G(τ). Starting with free two- or three-dimensional diffusion of a single species, the autocorrelation function can be modified adding intra-molecular photodynamic processes, introducing additional molecular species with different mobility, or considering obstructed 'anomalous' diffusion. Typical sources of fast intra-molecular fluctuations are excitation intensity dependent transitions of the dye to the long-living first excited triplet state and other less well-defined dark states, but also fluorophore isomerization, and reversible protonation [8, 9, 11, 23]. An exponential decay factor ($1 - T + Te^{-\tau/\tau_T}$) with the relaxation time τ_T corresponding to the triplet relaxation time, and the triplet fraction T of dark molecules, has to be introduced to account for these additional fluorescence fluctuations (Scheme 1).

Fluorescent dyes can also show distinct intra-molecular transitions between two or more differently bright states, e.g. a fast triplet transition and a slow on-off blinking, which have to be accounted for by an individual decay term for each transition. Figure 1 illustrates how autocorrelation curves change their shape due to intra-molecular transitions.

The local concentration of fluorescent molecules $\langle C_i\rangle$ can be determined for single species from correlation-curve amplitudes G(0) (extrapolated for $\tau \to 0$) (Scheme 1). Particle numbers N are proportional to inverse autocorrelation amplitudes G(0). If particles show a non-Brownian diffusion due to corralling or particle interaction with fixed structures, as has been described within membranes (2D) and cells an anomalous diffusion model can be applied to fit the data (Scheme 1) [24–26]. The autocorrelation function for anomalous 3D diffusion is

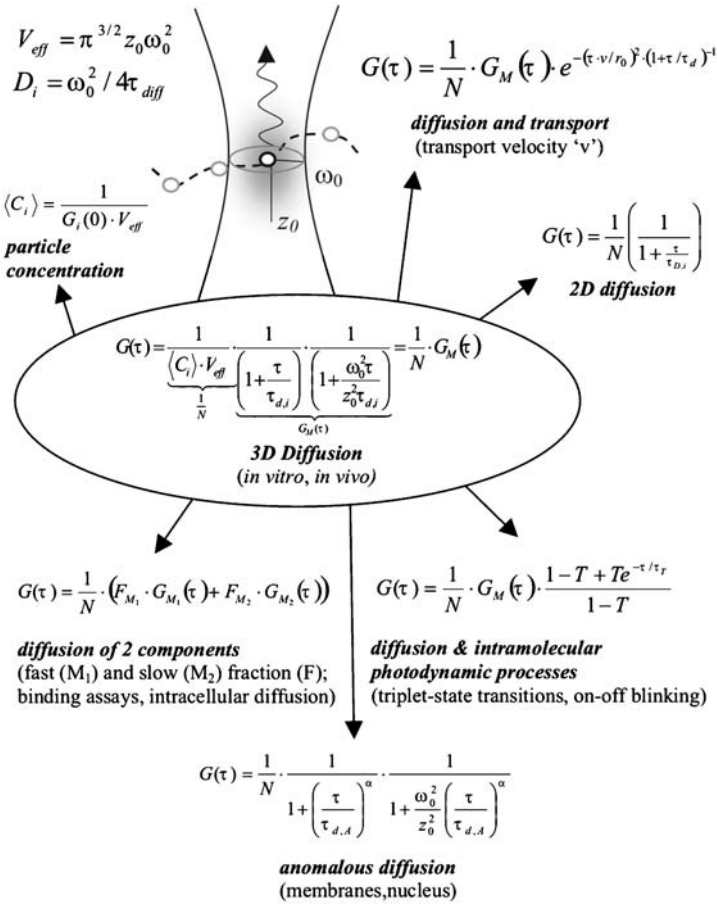

Scheme 1 Fitting functions for FCS analysis. Basic fitting functions and scheme for particle diffusion through the focal volume. Many experimental situations require combinations of the presented models. The complexity of a model to be applied is limited by the signal-to-noise ratio of recorded fluorescence fluctuations and the number of well-known parameters that can be fixed prior to analysis. The *grey shading* of the focus indicates the extension of V_{eff} and the Gaussian intensity distribution of the laser light within the focus

adapted by introducing an anomaly coefficient α indicating the degree of obstruction.

2.2 Cross-Correlation Analysis

Instead of autocorrelating a single signal trace, different signal traces originating from at least two spectrally different dyes within the same confocal volume element can be compared at high temporal resolution in a cross-correlation

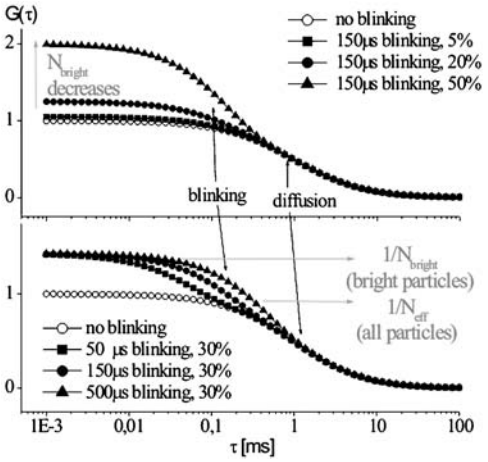

Fig. 1A, B Blinking in diffusion curves. The effect of blinking is visualized: **A** for an increasing dark fraction [%] and a fixed blinking decay time [µs]; **B** for a constant dark fraction and increasing blinking decay times. The number of bright particles decreases upon blinking, while the number of all detected particles stays constant (N=1). The correlation function acquires an additional shoulder and changes its shape. Diffusion takes place with τ_d=1 ms for all curves

mode (Fig. 2). Different dyes are either excited with two overlapping laser beams or TPE while fluorescence is collected in overlapping detection volumes of two separate detection pathways [27]. This way of analysis quantifies the degree of similarity between fluorescence fluctuations obtained from different dyes, and relies on fluorescence events that take place simultaneously. Only concomitant movement of spectrally different dyes accounts for cross-correlating fluctuation signals. Phenomena constricted to each individual fluorophore, like triplet-blinking, occur independently in each detection channel and do not contribute to the cross-correlation curve. The cross-correlation function for two diffusing species "i" and "j" of different colours is defined as

$$G_{ij}(\tau) = \langle \delta F_i(t)\, \delta F_j(t+\tau)\rangle / \{\langle F_i(t)\rangle \langle F_j(t)\rangle\} \quad (3)$$

The concentration of double-labelled substrate molecules can in ideally calibrated setups be easily determined from the auto- and cross-correlation amplitudes as shown in Fig. 2, since the cross-correlation amplitude is directly proportional to the number of double-labelled particles in V_{eff}. The percentage of double-labelled particles is thus given by the relative cross-correlation amplitude.

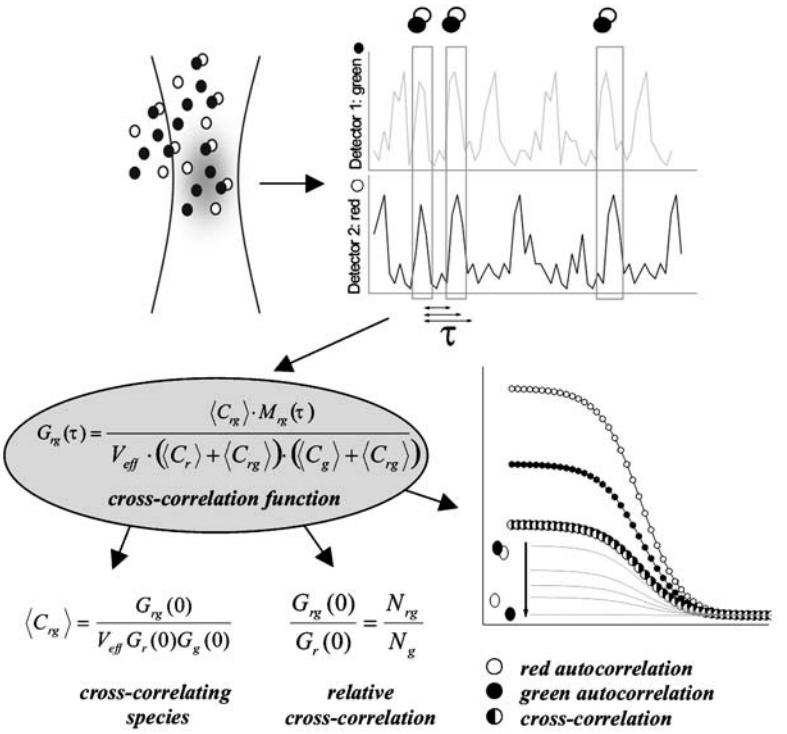

Fig. 2 Auto and cross-correlation analysis. Two traces of fluorescence fluctuations result from diffusion of single and double-labelled particles through V_{eff}. Simultaneous events in both channels have been highlighted in boxes and give rise to a cross-correlation amplitude $G_{rg}(0)$. Separation of connected labels results in a decrease of the cross-correlation amplitude while autocorrelation amplitudes stay constant. Changes in the number of double-labelled particles can be quantified both in absolute values $\langle C_{rg}\rangle$ and the relative cross-correlation

3 From Synthetic Dyes to Fluorescent Proteins

Single-molecule optical analysis relying on fluorescent dye molecules imposes stringent requirements such as high signal-to-noise ratios and steady photon fluxes for each observed molecule. Apart from high quantum yields and large absorption cross sections, fluorophores thus have to display a high photostability at up to several 100 kW/cm^2 laser intensities. It has been assumed that a conventional dye molecule emits about 10^5 to 10^6 photons before being irreversibly bleached [28] which corresponds to a maximum of several seconds of continuous excitation/emission for intensities applied with most single-molecule based techniques. Due to the high temporal resolution of modern optical methods, ideal dyes should also show a weak tendency for fast intra-molecular photophysical transitions to dark states, specified by singlet-to-triplet state

quantum yields and on-off blinking phenomena induced by pH or excitation light. Both, protein fluorophores and synthetic dyes were found to meet these requirements for single-molecule applications.

3.1 Protein Fluorophores Instead of Synthetic Dyes?

The selection of a suitable dye system crucially depends on the particle to be labelled (e.g. lipids, DNA, RNA, proteins) and whether in vitro or in vivo systems are to be examined. Both, chemical labelling by covalently linking small and activated organic dyes to biological molecules, and genetic labelling with fluorescent proteins in protein fusion constructs have been established as standard methods. Among the dyes that can be covalently linked to biological molecules and have been successfully applied in single-molecule based applications are rhodamine, cyanine, Bodipy and Alexa dyes. The expected chemical environment in a given application further specifies a dye's suitability, since either hydrophobic or hydrophilic dye properties have to be taken into account [29]. Moreover, not all dye molecules are equally suited for two-photon excitation. On the other hand, interactions of labelled molecules with their conjugated dyes can affect a dye's photophysical behaviour and have to be taken into account for assay design [30, 31]. Remarkably many synthetic dyes exhibit ~10 times slower bleaching kinetics as reported for protein fluorophores [32]. In contrast, a major disadvantage of applying synthetic dyes on biological molecules, particularly proteins, is the difficulty of labelling at a certain site and at a fixed molar ratio. Moreover, if to be applied in vivo, the labelled molecule has to be delivered into cells by microinjection, loading reagents, or electroporation, all of which introduce additional experimental handicaps and pitfalls.

Genetically encoded reporter constructs based on fluorescent proteins circumvent many of these problems. Proteins that may be hard to purify can be labelled and expressed intracellularly, and fusions readily be targeted to sub-cellular compartments. In addition, fluorescent proteins like EGFP are more or less inert in the cytosol and very rarely cause photodynamic toxicity [13, 14, 29]. Taken together, these advantages render protein fluorophores superior to synthetic dyes for most intracellular applications. The number of successfully applied fluorescent reporter constructs has significantly grown over the last years [12] (see Miyawaki within this issue). New fluorophores have been developed applying mutagensis strategies to known species, and have also been newly discovered in reef organisms. Naturally, not all fluorophores known to date are equally suited for single-molecule based approaches, and display common and individual advantages and limitations that will be discussed in more detail in this review. Recently, Zhang et al. and Miyawaki reviewed current trends and developments in finding fluorescent probes for cell biological research, addressing a large body of protein fluorophores, and practical details for their application [12, 13].

3.2 Fluorescent Proteins

With regard to future FCS applications based on fluorescent proteins, three questions have to be raised. First, which fluorophores have been successfully used for FCS so far? Second, which were their features? And third, which are interesting new candidate proteins for FCS analysis with appropriate photophysical and biochemical characteristics? In order to address these questions, a short overview of fluorescent proteins based on Table 1 will first be given.

3.2.1 GFP and its Mutants

Until recently, the green fluorescent protein (avGFP) from the jellyfish *Aequorea victoria* was the only fluorescent protein to be widely mutated and altered for biological applications. Meanwhile, a family of GFP-like proteins from different organisms has emerged that share the common β-barrel fold structure and intrinsic chromophores but represent a vast spectral range, with (E)GFP and DsRed being the most prominent representatives [33].

After wild-type avGFP had been optimised for proper folding at 37 °C and efficient expression within cells, efforts were directed to the design of spectral variants to allow for multi-colour applications of fluorescent proteins [34, 35]. When the protein has acquired its β-can fold, chromophore formation occurs autocatalytically by cyclization and dehydration of Ser-65, Tyr-66 and Gly-67 to a colourless and non-fluorescent imidazolone ring followed by oxidation to an extended conjugated system giving rise to fluorescence. Mutations have been inserted in and around the chromophore to alter spectral properties, being grouped into 7 classes [34]. Depending on its composition and neighbouring amino acids, the chromophore predominantly exists in either a protonated or deprotonated form, e.g. with a Tyr-66 phenol group or a phenolate, respectively. Although effectively shielded by the β-can, external pH shifts can lead to reversible chromophore protonation/deprotonation in most GFP variants, and shift their spectral properties.

As shown in Table 1, spectral variants with blue, cyan and yellow-green emission characteristics have been developed out of wtGFP and are now commercially available. Continuing efforts are made to improve fluorophore brightness and decrease their sensitivity against acidosis and Cl^- concentration, as with the third generation of YFP mutants, 'Citrine' and 'Venus', or the newly presented cyan-green CGFP [13, 36, 37].

Since GFP mutants emitting blue light have to be excited with near-UV lasers, they are less favourable dyes for sensitive intracellular applications due to the significant interference of UV radiation with cellular components. Nevertheless, advanced spectroscopic concepts such as three-photon excitation might shed new interest on blue fluorescent proteins, e.g. for combined two- and three-pho-

Table 1 A selection of fluorescent proteins and their properties

Name	Excitation/ emission maxima (nm)	Extinction coefficient ($M^{-1}cm^{-1}$)	Quantum yield (%)	Biophysical applications	Comments	Color	References
EBFP[a]	383/445	31,000	25	– No FCS reports – Low photostability	– Dim dye – Candidate protein for three-photon excitation	Blue	[107]
ECFP[a]	434/477	26,000	40	– No FCS reports – Tested less suitable for single-molecule microscopy	– Low photostability	Blue	[32, 107]
T-Sapphire	399/511	44,000	60	– No FCS reports – Largest Stokes shift reported for protein fluorophore – No pH-sensitivity	– New variant of the 'Sapphire' GFP mutant – Candidate protein for three-photon excitation – Fluorescence process involves an internal proton transfer	Green	[52]
EGFP[a]	489/508	55,000	60	– FCS – Single-molecule microspopy – (pH-dependent) blinking	– Most widely applied label due to its brightness and photostability	Green	[107]

Table 1 (continued)

Name	Excitation/ emission maxima (nm)	Extinction coefficient ($M^{-1}cm^{-1}$)	Quantum yield (%)	Biophysical applications	Comments	Color	References
MAG	492/505	41,800	80		– Reported monomeric mutant of AG – Native AG is a tetramer	Green	[53]
EYFP[a]	514/527	84,000	61	– FCS – Single-molecule microspopy – (pH- and intensity-dependent) blinking	– 'Citrine' and 'Venus' are improved versions with regard to photostability, reduced pH- and chloride-sensitivity	Green-yellow	[107]
PAGFP	505/525	–	–		– Photo-activable (413 nm) mutant of EYFP	Green-yellow	[50]
DsRed= drFP583	558/583	72,500[b]	68[b]	– FCS – Intensity-dependent blinking – No pH sensitivity – remarkably photostable in FCS	– Commercially available as DsRed1[a] – >20–30 h maturation time[b] – Obligate tetramer and aggregation – DsRed2[a]:threefold maturation speed, 68% brightness relative to DsRed1 – Aggregation tendency can be reduced	Orange-red	[11, 32, 39]

Table 1 (continued)

Name	Excitation/ emission maxima (nm)	Extinction coefficient ($M^{-1}cm^{-1}$)	Quantum yield (%)	Biophysical applications	Comments	Color	References
T1	554/586	30,100	42	– 36% brightness relative to DsRed1	– DsRed- Express[a] – Maturation half-time 0.7 h – Tetramer like DsRed1	Orange-red	[46]
tdimer2(12) (tandem)[c]	552/579	120,000	68	– FCS (see this review, intensity-dependent blinking)	– DsRed-mutant – Maturation half-time 2 h – Improved brightness	Orange-red	[42]
mRFP1 (monomer)	584/607	44,000	25	– FCS (see this review, intensity-dependent blinking) – Decreased photostability	– Monomeric, dim DsRed-mutant – Maturation half-time <1 h – Red-shifted compared to DsRed	Red	[42]
HcRed1[a] (dimer)	592/645	–	–	– FCS (see this review, intensity-dependent blinking)	– t-HcRed1 similarly bright as mRFP1 – Source for optimized far-red proteins	Red	[43, 108]
t-HcRed1 (tandem)	590/637	160,000	4				

Table 1 (continued)

Name	Excitation/ emission maxima (nm)	Extinction coefficient ($M^{-1}cm^{-1}$)	Quantum yield (%)	Biophysical applications	Comments	Color	References
EqFP611	559/611	78,000	45	– FCS – Intensity-dependent blinking – Large Stokes shift	– Tetramer, dissociates at high dilution – Intracellular maturation: ~6 h at 28 °C; none at 37 °C	Red	[78]
KAEDE	508/518 572/582	98,800 60,4000	80 33	– Emission switch from green to red after UV illumination	– Tetramer – Quantum yield is pH resistant	Green→ red	[51]

EBFP: Enhanced Blue Fluorescent Protein; ECFP: Enhanced Cyan Fluorescent Protein; EGFP: Enhanced Green Fluorescent Protein; EYFP: Enhanced Yellow Fluorescent Protein.

[a] Available from Clontech, Palo Alto, USA.

[b] Reported values show large discrepancies probably due to different protein purity and maturation (Baird 2000; Matz 1999; Patterson 2002; Campbell 2002).

[c] 'Tandem' indicates that two monomers have been fused to produce a one peptide chain dimer, while 'dimer' or 'tetramer' indicates that the protein is an obligate oligomer.

ton excitation in multicolour applications. So far, no mutant of Aequorea GFP exhibits emission maxima longer than 529 nm although there is a tremendous need for red-shifted fluorescent indicators also in single-molecule based approaches: Multi-colour applications require efficient spectral separation of fluorescence from different maximally bright fluorophores, and longer wavelength excitation/emission properties of the red-shifted dyes move them further away from the spectral regime where autofluorescence is present.

3.2.2 Red Fluorescent Proteins (RFPs)

The discovery of a naturally red fluorescent protein in *Discosoma sp*. named DsRed (drFP583) suddenly made red-shifted protein tags available, and started analogous intense efforts to optimise DsRed [38]. While only sparse dimerization of wtGFP could be observed and easily be eliminated DsRed is an obligate tetramer [39, 40]. Therefore, DsRed is likely to tetramerize any of its fusion partners and also shows the tendency to form aggregates possibly conferring cellular toxicity [13]. To eliminate this problem, both non-aggregating tetrameric mutants and also a dim monomeric version of DsRed, named mRFP1 (Monomeric Red Fluorescent protein 1) have been generated, reducing basic-acidic surface interactions between monomers [41, 42]. Also, dimerization of monomers in tandem fusions has been presented as a strategy to reduce and suppress oligomerization and aggregation [42, 43].

As a further drawback, native DsRed also exhibits slow and complex fluorophore maturation due to an additional autocatalytic modification, extending the chromophore's conjugation system and allowing for red fluorescence [44, 45]. Non-mature protein with 475-nm excitation/500-nm emission maxima transforms into mature protein with 558-nm excitation/585-nm emission maxima and requires >48 h to reach 90% of maximal fluorescence [39]. Fluorophore maturation has been significantly accelerated in a number of mutants, e.g. T1, mRFP1 and E57 and was proposed to depend upon the space around the fluorophore [46, 47].

Unfortunately, no monomeric bright red fluorescent protein with photophysical properties similar to GFP mutants or the tetrameric red proteins has been reported to date. Applying RFPs thus still requests one of three possible compromises: 1) using bright obligate tetramers with accelerated maturation and easily-reduced tendency for higher aggregation, 2) applying comparatively dark monomers, 3) applying RFP tandem fusions.

Apparently, strategies developed to abolish tetramerization and enhance brightness will have to be combined to yield the ultimate red protein tag, since all Anthozoan GFP-like proteins known to date seem to form obligate tetramers [33]. The presented drawbacks of red fluorescent proteins do not categorically preclude their use in intracellular applications and single-molecule based technologies, as shall be discussed in this review. Moreover two indirect strategies have been proposed to improve DsRed applications: pulsed expression of DsRed

enriched mature DsRed within cells and reduced spectral ambiguities, while co-expression of dark DsRed mutants titrated bright DsRed tags and reduced oligomerisation of tagged proteins [48, 49].

Two additional fluorescent proteins have to be mentioned in this section, because they provide exciting features for cell biology and also insight into the complexity of chromophore maturation. Patterson and Lippinicott-Schwartz [50] recently presented a photo-activatable YFP mutant (PA-GFP) that was found to increase fluorescence 100-fold after intense irradiation with 413 nm. Even more impressing, a green fluorescing protein from the stony coral *Trachyphyllia geoffroyi* had been cloned that emits bright green fluorescence after synthesis but switches to bright and stable red fluorescence upon UV illumination [51]. The protein was termed "Kaede" and unfortunately also forms a tetrameric complex.

3.2.3
Alternative Fluorescent Probes

Recent developments of alternative fluorescent probes have been reviewed by Zhang et al. and will be mentioned briefly in this review, pointing towards major promises and drawbacks for biological applications [13]. Griffin et al. reported specific covalent labelling of recombinant protein molecules inside live cells based on the formation of covalent complexes between a biarsenical dye (e.g. FlAsH, ReAsH) and a tetra-cysteine motif fused to proteins [54]. The method combines the advantages of site-specificity, by genetic introduction of the tetra-cystein motif, and the usage small synthetic dyes of different fluorescent emission [55]. Nevertheless, significant background staining and the necessity of delivery protocols for biarsenic dyes impose significant disadvantages. A different approach to design new fluorophores was presented by Bae et al. [56]: the fluorescence properties of a GFP mutant were changed by 'selective pressure incorporation' (SPI) of an amino acid analogue within the GFP chromophore in auxotrophic *E. coli* host strains. So far, the method is extremely difficult to apply within mammalian cells and only produced very wide emission spectra.

3.3
Applying Fluorescent Proteins as Tags

The application of fluorescent proteins as tags raises various questions about their general suitability as fusion partners. Its hard to predict whether tagging with a globular ~30 kDa domain will affect the function and native intracellular distribution of the protein of interest, and by which means, e.g. optimised intervening protein linker sequences, artificial effects can be minimized. Classical biochemical approaches like two-hybrid systems for mapping molecular interactions of random fusion proteins succeeded in spite of the apparent sterical limitations. Considering the enormous number of tagged proteins in

sensitive FRET studies, starting with calmodulin and more recently applying protein kinase B (Miyawaki et al. 1997; Calleja et al. 2003) proves that essential protein characteristics might not even be affected by tagging with two protein fluorophores [57, 58]. On the other hand, obligate fluorophore oligomerization like DsRed tetramerization results in untypical molecular constellations. This can affect the function of a tagged protein or be disadvantageous for the optical technique to be applied. Consequently, researchers have to provide evidences for proper protein function in both a molecular and cellular context, at best by gene replacement and reconstitution or alternative less elaborate approaches [59]. The question of how to fuse fluorescent proteins to proteins of biochemical interest has been addressed by several publications and proved to be worth considering [13, 60–63]. Apart from standard N- or C-terminal tagging, protein fluorophores were successfully inserted into other proteins of interest, and vice versa. Both fusion partners retained their native function or purposely showed altered fluorescence properties. Only weak fluorescence quenching of protein fluorophores attached to other proteins has been reported, e.g. 80% average brightness values of in vivo EGFP for an adenylate kinase-EGFP fusion protein [15]. This may result from steric and chemical protection of the chromophore within a rigid β-barrel. Moreover, intracellular expression systems can be tuned to produce fixed and reproducible ratios of different protein fusions which is highly advisable for dual colour applications. While the fluorophore ratio is fixed when expressing bi-coloured fusion-proteins, simultaneous expression of two separate fusions can be facilitated using internal ribosome entry sites in bicistronic gene arrangements [64]. Intracellular expression of fusion proteins also allows for fine tuning expression levels within the concentration range of 10 nmol/l to 1 μmol/l typically used for intracellular FCS analysis. Particularly low expression levels that mimic physiological conditions have been attempted applying linearized plasmids in transient expression [15] and inducible ecdyson or tetA based expression systems [65, 66].

4
Properties of Fluorescent Proteins Analysed by FCS

4.1
Photodynamic Processes Affect the Applied Method

Fluorescent proteins are nowadays ubiquitous in microscopic experiments, usually being imaged in fusion to cellular proteins at different levels of spatial and temporal resolution. Quantitative standard biological assays have been performed at the bulk level [67] depending mainly on the spectroscopic properties of autofluorescent proteins. These approaches have been addressing protein localization, gene expression, trafficking, sensitivity to local environment such as pH, and issues amendable to FRET (Fluorescence Resonance Energy Transfer), like Ca^{2+} sensing or protease reactions [57, 68]. Fluorescence Lifetime

Imaging Microscopy (FLIM) based approaches have presented intracellular FRET studies for conformational changes and protein-protein interactions and can be performed with high temporal resolution at the bulk level [58, 69]. In parallel, fluorescence-based imaging has increasingly been applied to the direct observation of single molecules to address their intra-molecular dynamics along with translational mobility both in vitro and in vivo [70–72]. Cellular autofluorescence decreasing S/N ratios and the choice of appropriate dyes showed to be critical to these studies [32]. Nearly all protein fluorophores analysed at the single molecule level unveiled unexpected properties such as reversible photobleaching and on/off blinking in microseconds to seconds time ranges [8, 73, 74]. These characteristics have important implications for studying single-molecule trajectories or intramolecular dynamics such as conformational changes.

In contrast to monitoring one molecule at a time in single-molecule microscopy, fluorescence correlation spectroscopy (FCS) combines single molecule sensitivity with averaging over a larger number of dyes, continuously diffusing in and out of the detection volume. This approach to single molecule analysis proved capable of efficiently discriminating intramolecular photodynamics from translational dynamics in a highly quantitative manner and is less sensitive to the long-living dark states reported for GFP [8, 10, 11, 73, 74]. Recent publications on FCS have documented its capability of tolerating autofluorescence and blinking phenomena, and their quantitative inclusion in data evaluation [6, 8, 9, 11].

4.2 EGFP, YFPs and DsRed analysed by FCS

Thorough photophysical FCS analyses have been carried out on various fluorescent proteins so far: EGFP, YFPs, DsRed. These studies produced valuable information for fluorophore usage as fusion partners and successive data evaluation. They also document which photophysical parameters of reporter molecules ought to be determined in vitro to reduce the number of unknown parameters in vivo. We briefly outline these fluorophore studies and continue to hint to implied options and limitations.

4.2.1 EGFP

EGFP differs from wtGFP in 4 amino acids, of which F64L improves folding at 37 °C and S65T was introduced to favour the deprotonated (phenolate) bright form of the chromophore, formed autocatalytically from Ser-65, Tyr-66 and Gly-67 [34]. FCS analysis after excitation with 488 nm unveiled that the EGFP chromophore shows a complex protonation equilibrium between 3 chromophore species, 2 protonated dark and one deprotonated bright state [8]. Due to characteristic (de-) protonation time constants, the chromophore exhibits

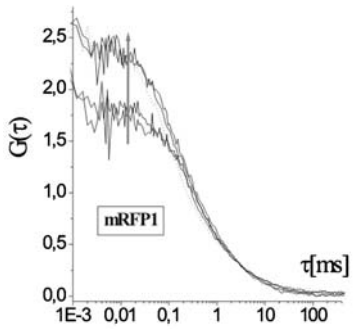

light intensity η *[kHz]* τ_d
5kW/cm² 2.9 cpm 1.4ms
4kW/cm² 2.1 cpm 1.3ms
2kW/cm² 1.9 cpm 1.2ms
1kW/cm² 1.1 cpm 1.5ms
7kW/cm² 3.8 cpm 1ms (dotted line)

A

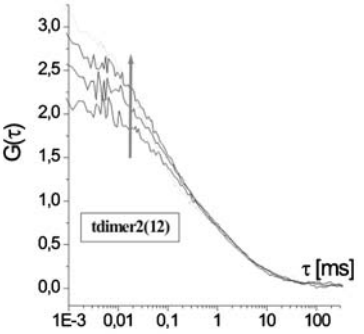

light intensity η *[kHz]* τ_d
13kW/cm² 8 cpm 2.0ms
8kW/cm² 3 cpm 2.7ms
5kW/cm² 3 cpm 2.0 ms
26kW/cm² 6 cpm 2.3ms (dotted line)

B

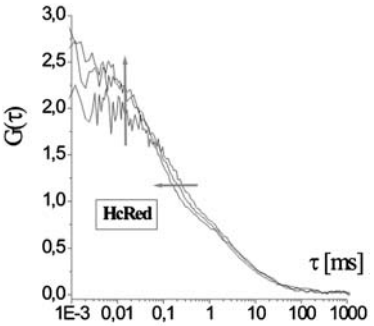

light intensity η *[kHz]* τ_d
10kW/cm² 3.5cpm 3ms
7kW/cm² 2.1cpm 3ms
5kW/cm² 1.9cpm 4ms

C

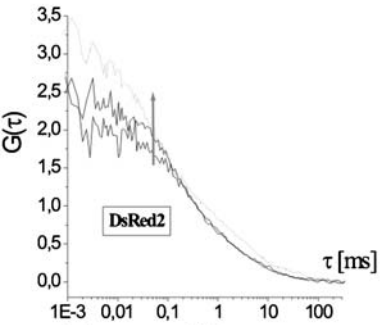

light intensity η *[kHz]* τ_d
8 kW/cm² 1.9cpm 3.4ms
5 kW/cm² 1.6cpm 2.3ms
16 kW/cm² 4.5cpm 4.0ms (dotted line)

D

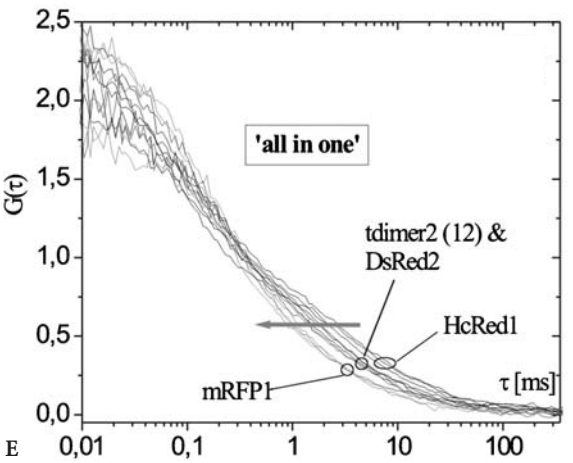

E

blinking that leads to specific contributions to EGFPs autocorrelation curves as shown in simulated curves in Fig. 1. The blinking relaxation times have been called chemical decay factor τ_C and increase from 50 µs to 450 µs upon a shift from pH 5 to 7 due to proton exchange with the solvent. The dark fraction F_C increases for low pH values (≈80% at pH 5). From pH 8 to 11 a ~13% fraction of the fluorophore shows pH independent blinking with τ_B≈450 µs that is due to internal protonation and slightly sensitive to excitation power. Apparently, a fitting function including only one exponential decay term was sufficient to describe these blinking phenomena within the tested pH range. With higher laser powers EGFP correlation curves showed an additional contribution (≈30 µs) that was assigned to triplet state population.

Interestingly, a Y66W GFP mutant lacking a protonable hydroxyl on the chromophore was examined by Haupts et al. (1999) and no pH-dependent fast fluorescence blinking detected [35]. In reverse, pH-sensitive GFPs can be applied as highly accurate pH sensors for in vivo applications read out by imaging methods or FCS [8, 75]. FCS applications in the cytosol take place at pH~7 and thus face little pH dependent blinking [76]. It is advisable to determine blinking parameters for the expected pH range before the evaluation of intracellular measurements. Also, application of GFPs in cases such as cellular acidosis, e.g. within hippocampal neurons, requires consideration of blinking phenomena and might be simplified by usage of pH-resistant mutants like "Sapphire" unless they have to be applied as pH sensors [34, 52].

4.2.2 YFPs

In analogous studies, the yellow-shifted GFP mutants S65G/S72A/T203Y, S65G/S72A/T203F and Citrine showed both, pH-dependent and excitation intensity-dependent blinking [9, 10]. The flickering rate increased with excitation

Fig. 3A–E Comparison of RFPs in the cytosol of Hek293 cells. Autocorrelation curves were recorded at different excitation intensities, normalized and plotted for: **A** mRFP1; **B** tdimer2(12); **C** HcRed1; **D** DsRed2; **E** superimposed to allow for visual comparison. Diffusion properties (τ_d in 'ms') and particle numbers (used for normalization to N=1) could be determined and revealed molecular brightness values (η given in 'counts per molecule' [kHz]). *Dotted lines* (A, B, D) represent atypical diffusion curves attributable to bleaching. According to our interpretation, dark fractions increased for all tested RFPs from ~40% to ~60% (indicated by *vertical arrows*) with growing intensities (543 nm) that were determined before entering the microscope. Diffusion curves (E) suggested significant differences in particle mobility (indicated by *horizontal arrows*, E). While mRFP1 seemed to show the highest intracellular mobility (E, B) tdimer2(12) performed as the brightest dye (A) in our measurements. In contrast, mRFP1 (B), DsRed2 (C) and HcRed1 (D) showed photobleaching even at fairly low intensities. DsRed2 (C) and HcRed1 displayed a slow second diffusing component that made curve fitting rather difficult and favoured bleaching. This comparison of dynamic RFP-behaviour within cells fits well with their biochemical characterization and predicted behaviour

intensity, accordingly the decay time decreased with τ_B<100 µs, showing a constant dark fraction of F≈60%. A second dark state (10–100 µs) resulting from chromophore protonation could be observed below pH 8. Thus YFPs required two exponential decay terms with τ_C and τ_B to fit data of the low to moderate pH measurements.

4.2.3 DsRed

DsRed displays both chemically and photophysically remarkable features. In FCS, its strong light-dependent blinking seems to involve three different fluorophore states, at least two of which are fluorescent [10, 11]. Two characteristic fluctuation time scales $\tau_{D(1)}$ and $\tau_{D(2)}$ reaching from several tens to several hundreds of microseconds with intensity dependent dark fractions D_1 and D_2 were assigned to conformational rearrangements of the chromophore. Moreover, the fluorescence spectrum of DsRed red-shifts ≈8 nm after increasing excitation intensity. In contrast to most GFP mutants, the DsRed fluorophore doesn't show any pH-dependent blinking for pH 6 to 11. Upon two-photon excitation, the light-dependent flickering was not detected and DsRed seemed to be remarkably photostable. Obligate tetramerization of DsRed and formation of higher order aggregates could be detected by FCS analysis even at low nanomolar concentrations since ~1.5- and ~2.4-fold lower diffusion coefficients (~4- and 13-fold larger MW) compared to monomeric GFP have been determined for purified DsRed. The nature of fluorescence emission of DsRed has also been addressed in single-molecule analysis with important implications for FCS [77]. Monomers within a tetramer were proposed to transfer energy between each other. In consequence, emission results with equal probability from each of the four chromophores. Thus, an excitonic mode of excitation transfer seems to be active, while independent emission from individual monomers can be excluded.

86% of DsRed tetramers were found to contain at least one immature green monomer. Consequently, DsRed tetramers present an inhomogeneous population of dye molecules that show high sensitivity to excitation intensities due to complex energy transfer processes among the monomers. The resulting complexity and heterogeneity of emission behaviour implies that FCS analysis offers a rather phenomenological description of DsRed fluorescence and is therefore well suited to analyse particle numbers and mobilities. No similar blinking phenomena as reported for DsRed has been described for monomeric GFP mutants.

A new red protein eqFP611 from *Entacmaea quadricolor* displayed both monomeric and tetrameric features in initial studies [78]. FCS analysis at low nmol/l concentrations predicted a mass ratio of 2.7 between DsRed and eqFP611 and produced a diffusion coefficient similar to the monomeric GFP mutant Citrine. In contrast, size-exclusion chromatography and the recently resolved crystal structure of eqFP611 indicated that eqFP611 too can form tetramers

based on extensive monomer surface interactions [79]. Interestingly, six mutated residues in the monomeric DsRed variant mRFP1 can also be observed at the corresponding positions of eqFP611. Thus eqFP611 seems to be a promising substrate for mutational optimisation of its features, e.g. shifting its maturation optima from 24.5 to 37 °C and decreasing its oligomerization tendency.

4.3 On-Off Blinking of Protein Fluorophores in FCS

Because dark fractions of blinking protein fluorophores appear in steady state fluorescence measurements as a reduced quantum yield and efficiency, they can reduce a fluorophore's potential as a fluorescent marker. In part, this limitation can be counterbalanced by time-resolved FCS. If the blinking decay time τ_B gets however too close to the diffusional decay times τ_d or even larger, the number of fluorophores present in V_{eff} could be significantly underestimated in the case of large dark fractions. This effect would also decrease the maximum cross-correlation amplitude to be expected in dual colour cross-correlation analysis. Thus, blinking can set a lower limit for V_{eff} and resulting diffusion times, unless underestimation of particle numbers can be tolerated. To separate blinking from diffusional fluctuations, different sizes of V_{eff} can be readily compared. The application of TPE seemingly eliminates intensity-dependent blinking in most fluorescent proteins, due to different selection rules. Here also, intensity dependent photoconversion to long-living non-emitting states can also reduce apparent diffusion times analogously to photobleaching, and can easily be detected applying different intensities.

In summary, FCS can quantitatively account for blinking phenomena that proved to be common to frequently used fluorophores. Interestingly, the fraction of intensity dependent blinking seems to increase with red-shifted emission of protein fluorophores. It is tempting to speculate whether this might be due to the extended π-electron systems present in red fluorescent dyes.

4.4 Fluorophore Oligomerization, Aggregation and Dim Fluorophores

Fluorophore aggregation can occur by self-aggregation of fluorophores (see above), but also in fusions to oligomer-forming partners, and affects FCS data evaluation. Oligomerization of fluorescently tagged proteins leads to a distribution of molecular brightness that has to be considered for proper determination of particle numbers [16, 21]. There exist several methods of choice to examine the accurate distribution of monomeric vs oligomeric molecules that can be applied on the same data sets used for FCS analysis: Fluorescence Intensity Distribution Analysis (FIDA) and Photon Counting Histogram (PCH) analysis both consider intensity distributions in fluctuation traces [80, 81]. Fluorescence Intensity Multiple Distributions Analysis (FIMDA) combines fea-

tures of FCS and FIDA, allowing for simultaneous determination of molecular brightness and diffusion times [82]. Besides that, an FCS based approach to analyse polydispersity has been presented and higher-order autocorrelation introduced [83, 84]. Singular bright particles that present a significant or dominating contribution to the correlation curve usually have to be excluded from FCS analysis by running short repetitive measurement intervals to select and average only traces devoid of aggregates [22].

Mutant fluorescent proteins optimised for shifted fluorescence excitation/emission properties or fast maturation and weak oligomerization (DsRed mutants) often display very low molecular brightness values due to photobleaching or small quantum yields. Figure 3 presents an initial attempt to measure and compare autocorrelation curves of DsRed2 and its mutants tdimer2(12) and mRFP1 as well as HcRed1. The application of comparatively dark red fluorophores in vivo takes advantage of the decreased cellular autofluorescence in the red compared to the green emission range (see below). It requires an adaptation of the experimental setup, like applying TPE or varying the size of the laser focal spot, both affecting local molecular brightness and 'signal to noise' ratios (see discussion in this review).

4.5 Photobleaching and Photostability

Sufficient photostability of dyes is an important prerequisite for FCS studies in general and particularly inside live cells. Photobleaching affects both auto- and crosscorrelation amplitudes and introduces a significant artefact risk in FCS analysis [16, 21]. Moreover, cells of several picoliters volume will contain only 10^5 to 10^6 dye molecules at dye concentrations of 10–100 nmol/l and thus are readily subjected to dye depletion. As reviewed here, EGFP, various YFPs and RFPs have been found to work well with FCS applications displaying sufficient brightness and photostability. Photophysical properties of autofluorescent proteins have been compared for ECFP, EGFP, EYFP and DsRed [32]. ECFP seems less suited for FCS due to its low brightness and high susceptibility to photobleaching, while EYFP was shown to be equally suited as EGFP. Despite its strong excitation-dependent blinking, DsRed was found to exhibit very little photobleaching in FCS analysis within an excitation intensity range of 0.5–100 kW/cm^2 and long measurement intervals [11]. In contrast, low photostability of DsRed and DsRed-mutants has been reported, although Harms et al. indicated that dark states complicate the interpretation of photobleaching data [32, 42]. In addition, ECFP, EGFP, EYFP and DsRed were shown to be excitable by two-photon excitation [85].

4.6
Two-Photon Excitation of Fluorescent Proteins

Two photon excitation (TPE) and its application to FCS analysis has been described and discussed in detail and shall be briefly reviewed with regard to fluorescent proteins and intracellular usage [6, 7, 86, 87].

Two-photon excitation requires quasisimultaneous (10^{-15} s) absorption of two photons of approximately double the wavelength as usual and thus is limited to a small self-confined volume element displaying sufficiently high photon flux densities. High photon flux rates are usually provided by employing pulsed laser systems. TPE confers particular advantages to intracellular applications, since both cell damage and sample depletion by photobleaching are significantly reduced and limited to a small focal spot compared to one-photon excitation taking place throughout the created light cone. Consequently, TPE was applied for long-term data acquisition of TMR in live cells without significant loss of fluorescence signal [6]. TPE of the protein fluorophores ECFP, EYFP, EGFP and DsRed has been examined and excitation cross-spectra have been recorded, while TPE FCS has been performed on rsGFP, EGFP and DsRed [6, 14, 85, 88]. Intersystem crossing to intensity-dependent dark state is typically much less likely since different photophysical transitions are involved in TPE.

Due to these different selection rules for excited fluorophores, TPE spectra of different dyes can show significant overlap in contrast to their one-photon excitation spectra. Consequently, both synthetic and protein fluorophores with largely different emission have been efficiently excited with a single IR laser line in TPE based cross-correlation studies [7, 17, 88]. Analogous three-photon excitation with IR lasers requiring ~10-fold higher intensity densities allows for exciting UV-absorbing dyes and might be used in combination with TPE [89].

5
Single Colour Applications of Fluorescent Proteins In Vivo

The number of intracellular FCS applications based on fluorescent proteins is constantly increasing. Single colour applications can provide data about the localization and concentrations of fluorophores and their fusions, intramolecular photo-dynamics and particle mobility.

5.1
Concentration Measurements

FCS allows for highly precise and locally confined determinations of particle concentrations, that help to monitor and correlate genetic and physiological processes within cellular compartments, as was demonstrated within *E. coli*, the only reported FCS application within bacteria to our knowledge [90].

5.2 A Sensor for Environmental Conditions

With regard to its pH sensitivity, GFP in combination with FCS is considered an intracellular pH sensor [8–10]. Internal calibration even within cells can be performed by examining both particle numbers and photophysical dynamics in parallel, and pH-sensitive protein fluorophores can efficiently be targeted to different cellular compartments [75]. Another interesting approach, though not necessarily depending upon FCS, consists in the insertion of allosteric sites into protein fluorophores that influence fluorescence properties upon ligand binding [13, 63].

5.3 Mobility as a Precise Measure of Particle Action

Determination and comparison of particle mobility can shed light on all events affecting particle motion. This can account for particle interactions such as protein-protein interactions and ligand binding, particle partitioning into different cellular compartments or active transport phenomena.

5.3.1 Active Transport

Depending on the characteristic shape of autocorrelation curves, active transport of GFP in vivo could be distinguished from diffusion within plastid tubules of plant cells and its properties described in more detail [91]. Bright GFP batches and not single molecules were actively transported in a plug flow mode, while laminar flow could be excluded. The approach of this study can be applied to any other elongated narrow structure, like dendrites. Even more powerful, FCS strategies presented for the analysis of fluorescent particles in microstructures, like applying two laser foci and examining spatial cross-correlation, can as well be transferred to organic structures [92].

5.3.2 Diffusion: A Comparison off In Vitro and In Vivo Applications

Assessing changes in particle size on the basis of diffusion times derived from FCS measurements has been successfully accomplished in a number of in vitro binding experiments and was initially applied to study quantitative hybridization kinetics of DNA probes to RNA [93, 94]. Moreover, a detailed and systematic examination of autocorrelation analysis of ligand-protein binding equilibria has been presented, and the handling of brightness distributions arising from oligomerization of labelled monomers has been discussed [81, 83, 95].

However, autocorrelation analysis offers a limited resolution for two-component solutions (e.g. free ligand, bound and slower ligand) since the diffusion

time scales only with the third root of the molecular weight of spherical particles. Thus, large mass changes result in comparatively small changes in τ_{Diff} and D_i. Meseth et al. determined a resolution limit at a minimum ratio of 1.6 in diffusion times τ_{Diff} for equally bright particles, which corresponds to a factor of 4 in molecular mass [96]. For less ideal conditions like different dye-brightness, a much bigger ratio for τ_{Diff} is required for proper separation of two components. With regard to the inhomogeneity of the intracellular environment (see below for discussion) and the stringent requirements described above, this kind of analysis, though very powerful for binding studies in vitro, won't be applicable to most in vivo situations.

Nevertheless, differences in mobilities of EGFP tagged proteins can be readily exploited to analyse partitioning in different cellular compartments like the cytosol and the plasma membrane, and to document changes in cellular localization [15, 97]. Molecules in the cytosol and the plasma membrane differ in their mode of diffusion (3D- and 2D-diffusion, respectively), and the degree of anomalous diffusion that has to be assumed to fit the obtained data. This experimental approach nicely tracks changes in localization and distribution of proteins involved in signalling from the plasma membrane to the cytosol and nucleus, and thus presents an efficient tool for analogous investigations.

In order to perform rigorous mobility analysis for in vivo situations, cell-type specific intracellular viscosities (see below) and a wide distribution of mobilities within the same compartment of a given cell have to be taken into account. Mobility analysis of EGFP in the cytosol of Hek293 and Hela cells resulted in quite similar values for $D_{EGFP} \approx 2.3–2.5 \times 10^{-7}$ cm^2/s but a lower value $D_{EGFP} \approx 1.3 \times 10^{-7}$ cm^2/s within AT-1 and Cos-7 cells [14, 15, 25, 97]; for comparison $D_{EPFP} \approx 8.7 \times 10^{-7}$ cm^2/s was determined in water. Thus, a comparison of fusion protein mobilities derived from different cell lines requires normalization to a reference control such as EGFP. Moreover, values for D_{EGFP} in the cytosol showed standard deviations of at least 10% for different measurement positions that have to be assigned to interactions with organelles and unknown particles, and make proper statistical approaches to mobility based in vivo studies obligatory. The exact position of the measurement volume V_{eff} within cells, in particular the proximity of membranes, can affect obtained mobility values. Nevertheless, extensive PCH and FCS analysis by Chen et al. excluded disturbing and detectable interactions of EGFP with intracellular compounds [14]. Comparing mobilities of EGFP and EGFP-fusions in the cytosol yielded intriguing implications about fusion protein behaviour: while some constructs showed the theoretically predicted difference in D_is according to molecular weight ratios another fusion protein moved much slower than predicted and showed a significantly larger mobility standard deviation [15, 25, 97]. This may account for a non-spherical conformation, or more interesting, for unexpected and specific interactions that are of particular interest for proteins involved in signalling. On the other hand, finding predicted D_is based on molecular weight ratios to a reference fluorophore confirms the absence of specific interactions and thus presents a nice internal mobility control.

Interestingly, diffusion behaviour in the nucleus was found to depend on the cell cycle: in metaphase nuclei it was comparable to the cytosol, while showing significantly different mobility properties in interphase nuclei [25].

Experimental data from in vivo measurements have been fitted both with multi-component models and assuming anomalous diffusion [6, 15, 25]. Certain applications like measuring in fragmented cell membranes clearly require anomalous diffusion models [24]. Applying either model automatically implies a slightly different explanation for the observed phenomena: for multi-component fits, the dye is supposed to partly interact and move together with slow particles. For anomalous diffusion, the dyes movement appears restricted by inert obstacles obstructing molecular motion by an excluded volume interaction which can even result in a confinement of the detection volume as within small cavities [25, 26]. Accordingly, Verkman recently reviewed solute and macromolecule diffusion in cellular compartments and described three factors accounting for slowed intracellular diffusion: 1) slowed diffusion in fluid-phase cytoplasm, 2) probe binding to intracellular components, and 3) probe collisions with intracellular components, called molecular crowding [98].

5.4 Practical and Theoretical Considerations for FCS on Protein Fluorophores In Vivo

5.4.1 Dealing with Background Fluorescence in Buffers and Cells

Several reports documented that FCS can accommodate fluorescent background quite well. This ranges from easy estimates based on negative controls to a formal mathematical treatment and inclusion into analytical formulas. Fluorescent background can be found within cells or buffers including fluorescent components such as Triton-X 100. Cellular autofluorescent molecules constitute a heterogeneous group including NADH, flavins and flavoproteins, collagen and elastin, lipofuscin and can be found throughout the cell. Its properties seem to depend on normal and transformed cellular conditions and metabolic activity [99].

Immobile or slow sources of autofluorescence will contribute an uncorrelated fluorescence signal and can easily be photobleached or corrected for mathematically [6]. The concentration of diffusible components contributing correlated fluorescent signals has been estimated to range between 0.3–15 nmol/l in the cytosol of mammalian cells and 23 nmol/l in the nucleus and also average molecular brightness values were determined in studies using different cell lines and modes of excitation [6, 14, 100]. Obviously, the collected cellular background is strongly dependent on chosen excitation/emission parameters, e.g. is a factor of 2 higher at 488 nm compared to 543 nm, and significantly lower for 2PE [6, 32]. Flavins in particular exhibit strong fluorescence emission within the detection range of EGFP and EYFP [32]. Blab et al. examined TPE cross spectra of flavin mononucleotide and concluded significantly smaller excita-

tion rates of flavin for TPE compared to one photon excitation [85]. As a rough estimate, Schwille et al. proposed to introduce background fluorescence into the autocorrelation function for fluorescence $F_{background}>0.1\ F_{total}$ and high molecular brightness $\eta_{Background}$ [6]. Strong background fluorescence otherwise could lead to an overestimation of the actual particle number and underestimation of molecular brightness values and also affect cross-correlation amplitudes. The relation of apparent and real particle numbers and brightness values can be described formally and help to correct data interpretation [14]. Particularly low nanomolar concentrations of reporter molecules in cells (<10 nmol/l) can require more elaborate data analysis, therefore intracellular concentrations for fluorescent proteins like EGFP should range within 10–100 nmol/l for convenient and reliable analysis [6]. Comparison of the molecular brightness of reporter molecules in vitro and in vivo which is linked to the apparent particle number can serve as a direct and easy measure for the impact of autofluorescence [6, 14]. When applying one photon excitation, the size of V_{eff} (primarily controlled by the pinhole diameter in the detection unit) has an important impact on background phenomena. With intensities well below the saturation threshold, the fluorescence collected from each dye molecule increases in larger detection volumes V_{eff}. Yet for one-photon excitation, the relative increase of the photon yield per detected molecule η in vivo is much smaller than in vitro, since the scattering background contribution is significantly favoured in larger volumes. Interestingly, nearly equal values of η in vitro and in vivo could be obtained after TPE for both synthetic dyes and EGFP which can be explained by the small excitation/detection volume collecting less background from autofluorescence [6, 14]. For one-photon excitation, a compromise between background contributions and molecular brightness needs to be found that allows for reliable data interpretation.

These initial 'signal to noise' considerations are particularly important with regard to the application of non-ideal dyes. They help to design appropriate negative controls and optimise the measurement system with regard to fluorophore excitation/emission maxima and dye concentrations. Theoretical brightness comparisons of different dyes can be readily accomplished for known absorption coefficients and quantum yields. Nevertheless, experimentally obtained molecular brightness values η depend dramatically on excitation, used emission filters, and V_{eff}. They can be low even for bright dyes if crosstalk has to be minimized in multicolour applications.

5.4.2 Choice of Cell Line

In the first place, the choice of a cell line depends on biological requirements of the system to be studied. However, it should be highlighted that with regard to intracellular particle mobility and the degree of autofluorescence, different cell lines can't necessarily be considered equal for optical methods with single molecule sensitivity. Slightly different compositions of the intracellular matrix

might severely affect autofluorescence and particle mobility, and thus the dye bleaching, due to their influence on average residence times. Comparing previous studies, the viscosity in the cytosol was found to be 2.6- to 10-fold higher than in aqueous solution [25]. The growing number of confocal applications allows for a comparison of highly accurate mobilities in so far used cell lines. Schwille et al. provide a very systematic study of particle brightness and mobility, including a comparison of cytosolic measurements with the dye CMTMR in Hela, EMT6 and RBL cells [6]. The investigated dye molecules display both different mobilities and partitioning to differently mobile fractions. Differences in EGFP mobility among different cell types have been addressed above. It can't be excluded that the standard deviation of mobilities within a single compartment also varies with different cell lines [6]. In summary, there are qualitative differences in viscosity and background fluorescence between different cell lines though these can only vaguely be quantified.

6
Dual-Colour Applications: Cross-Correlation Analysis

6.1
Different Applications of Cross-Correlation Analysis

The application of two spectrally distinct fluorophore tags within a given system allows for a much more detailed study of molecular interactions and molecule behaviour in general, than in one-colour experiments. Cross-correlation analysis presents a direct and precise measure for particle interactions. Moreover, simultaneously obtaining two autocorrelation functions provides data about particle numbers and mobility that present important internal reference and calibration parameters. Starting with the analysis of DNA hybridisation, the technique has been further evaluated in model systems addressing real-time enzyme kinetics and the exclusive application of protein fluorophores and has been successfully applied in vivo [3, 16, 17, 88, 101]. Studying events at the single protein level holds the biggest promise for in vivo applications. Degradative processes such as protease reactions will be typically described by decreasing cross-correlation amplitudes [88]. Specific and reversible protein-protein interactions can be illustrated by both decreasing and increasing cross-correlation amplitudes [17]. Cross-correlation analysis also can be applied to address phenomena of indirect particle interactions within complex aggregates and colocalization within small diffusing compartments, such as active transport or co-localization in endocytic vesicles smaller than V_{Eff} [16]. It seems that the case of decreasing cross-correlation amplitudes for degradation events, starting at a typical maximum amplitude, is somewhat easier to address, since maximum amplitudes of interactions at equilibrium are primarily unknown and require proper functioning of the tagged binding partners.

6.2 Comparing Cross-Correlation Analysis to FRET

Fluorescence Resonance Energy Transfer (FRET) presents a popular approach to study molecular interactions and conformational changes both in vitro and in vivo, and emerged as a promising spectroscopic tool to study single-molecule dynamics [57, 70, 102–104]. In FRET studies, molecular processes can be evidenced by spectral changes of the emission signal because of distance-dependent energy transfer from an excited donor dye to a long-wavelength acceptor, and additionally by determining decreased donor lifetimes in Fluorescence Lifetime Microscopy (FLIM) [105]. Hence, FRET has been used for the development of efficient intracellular ligand-binding and protease assays and also probed for protein-protein interactions and conformational changes in live cells [57, 58, 68, 69, 106]. However, FRET requires spatial distances between donor and acceptor dyes of typically 20–60 Å and thus faces a fundamental sterical limit reducing its versatility. Dual-colour fluorescence cross-correlation spectroscopy evades this limitation by only depending on concomitant signal fluctuations from a confocal detection volume in two spectrally distinct emission channels. FRET analysis itself provides no intrinsic calibration parameters like particle concentrations and dynamic particle properties.

6.3 Cross-Correlation Analysis Based Solely on Fluorescent Proteins

Obviously, finding an appropriate combination of two proteins for in vivo cross-correlation analysis would significantly simplify these studies. In addition to identifying protein fluorophores with high brightness and photostability, a small spectral overlap of fluorescence emission is required to minimize detector crosstalk, e.g. representation of a green dye's emission in the red detection channel. Depending on particle number and brightness ratios, strong detector crosstalk (>10%) results in a significant overestimation of double-labelled particle numbers, which can be corrected for by including 'crosstalk'-particles and their brightness into the correlation functions, analogously to polydispersity. Molecular blinking phenomena help to distinguish 'real' from artifactual cross-correlation, since the blinking shoulder is not present in real cross-correlation curves [21].

DsRed and its mutants display emission spectra sufficiently red-shifted for two-colour applications with GFP mutants. The only combination of GFP mutants to display a similar small spectral overlap is presented by EBFP and EYFP, but no FCS application of EBFP has been reported so far and its excitation maximum (388 nm) is unfavourable for intracellular applications.

Accordingly, Kohl et al. reported an in vitro protease assay for two-photon cross-correlation analysis based solely on the fluorescent proteins rsGFP and DsRed [88]. A GFP-peptide-DsRed construct named STEV-ST was purified and subjected to proteolysis separating the fluorophores. With regard to future

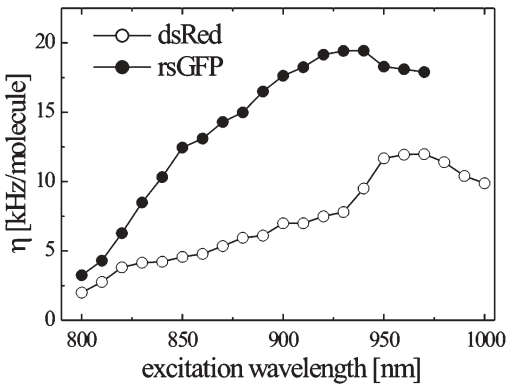

Fig. 4 TPE of GFP and DsRed. Wavelength dependence of the fluorescence emission yield η was determined for rsGFP and DsRed with two-photon-excitation. Photon yields per molecule were measured under conditions well below photobleaching. The optimal wavelength for joint excitation of both dyes was 940 nm with a maximum intensity of 20 mW

applications in live cells, simultaneous two-photon excitation of both fluorophores was attempted and efficiently realized at 940 nm with intensities safely below photobleaching (Fig. 4).

Equal dye brightness under the chosen conditions and minimized detector crosstalk of less than 10% presented convincing starting conditions for cross-correlation analysis based on rsGFP and DsRed. The proteolytic cleavage of STEV-ST was monitored by real-time FCS analysis as illustrated in Fig. 5a. Online kinetics of cleavage reactions at different enzyme concentrations were presented and allowed for easy discrimination of reaction rates depending on enzyme concentration. Moreover, the combinability of FRET and FCS analysis was demonstrated based on internal calibration by particle brightness values (Fig. 5b). The influence of FRET on cross-correlation analysis due to changing ratios of molecular brightness upon binding/unbinding of labelled particles could be quantified. In summary, sufficient proof of principle for protein-based dual-colour cross correlation analysis has been presented, along with an interesting extension of FCS to FRET phenomena.

6.4 Revisiting RFPs

Whether transfer of the dye pair GFP/DsRed or any analogous combinations to in vivo applications will work successfully depends on intracellular photon yields per molecule and the extent of fluorophore oligomerization. Nearly equal molecular brightness values for in vivo and in vitro situations were reported for EGFP implying that molecular brightness issues are unlikely to impede intracellular applications of the presented DsRed/GFP pair. Tetramerization of a reporter construct like STEV-ST devoid of any physiological role probably won't

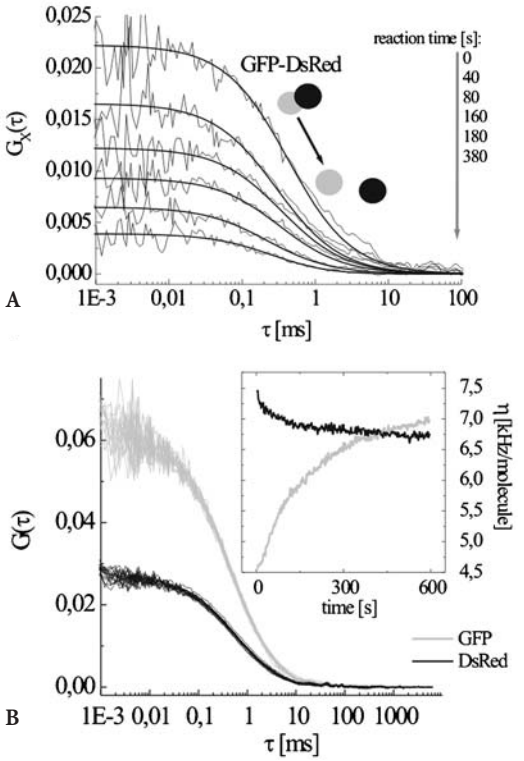

Fig. 5A, B Proteolytic cleavage analysed by: **A** cross-correlation analysis; **B** FRET on single-molecule-scale. In A, during the course of a specific proteolytic reaction GFP and DsRed get separated leading to gradually decreasing cross-correlation amplitudes $G_X(0)$ determined in 40-s intervals. In B, alternatively, autocorrelation functions and photon counts per molecule in kHz (*inset*) for rsGFP and DsRed were determined in parallel during a proteolytic digest. Changes in fluorescence intensity of FRET donor and acceptor were detected immediately after enzyme addition, whereas autocorrelation G(0) values and fluorescent particle numbers remained constant. The monitored increase of rsGFP fluorescence corresponds to approximately 35% FRET in the intact substrate

affect its function while presenting a delicate issue for protein-protein interactions in signalling. Remarkably, DsRed has been applied as the acceptor dye in several intracellular FRET studies addressing both conformational and protein interaction processes [58, 69]. Tetramerization only partly interfered with protein function, mainly by affecting cellular distribution. Nevertheless, DsRed fusions and DsRed alone were found to show variable behaviour in different cells, ranging from no detectable aggregation to punctate localization [48]. A wide distribution of oligomeric states up to high-order aggregates is rather obvious for visually punctate fluorescence and will impair protein function and FCS studies.

In summary, DsRed and its mutants represent interesting fusion partners for in vivo cross-correlation analysis although drawbacks cannot be excluded. Nevertheless, researches should consider the variety of DsRed mutants existing to date and evaluate compromises such as monomeric but rather dark (mRFP1) or bright but bulky dimeric tags such as tdimer2(12).

6.5 Cross-Correlation Analysis In Vivo

Performing cross-correlation analysis in vivo on genetically tagged proteins is most desirable since it avoids the need for any dye delivery and promises a highly quantitative characterization of all involved molecular species. The first cross-correlation studies in vivo based on external uptake of fluorescent molecules have been reported recently, simultaneously with the application of GFP and DsRed for in vitro cross-correlation analysis [16, 17, 88]. Thus, the next step of setting up a cross-correlation application solely based on fluorescent proteins in vivo is not far-fetched and shall be discussed on the basis of these studies.

So far, attempts to measure dual-colour cross-correlation in vivo rely on externally labelling at least one of the target molecules and introducing it into the cell. Studying endocytosis of fluorescent particles by FCS facilitates the issue of dye delivery and was accomplished to analyse the fate of A and B subunits of cholera toxin after cellular uptake [16]. Cross-correlation of the holotoxin consisting of the Cy2-labeled A subunit and the Cy5-labeled B subunit could be detected after endosomal uptake and was diminished significantly after the toxin had reached the Golgi. In this study, small endosomal vesicles constituted the diffusing entity as could be told from diffusional properties and particle brightness. A reduction in cross-correlation thus indicated that A and B subunits adopted individual pathways in vesicle trafficking. The study was performed using one photon excitation with two laser lines, applying the commercial Zeiss ConfoCor2 setup. Very high signal-to-noise levels could be obtained, which has been attributed to very bright diffusing particles, as the endocytic vesicles contained several fluorophores. Additionally, a thorough discussion of bleaching phenomena that can lead to artifactual cross-correlation is provided.

Another recent intracellular cross-correlation study succeeded in monitoring reversible protein binding. Using two-photon excitation, binding and unbinding of Alexa 633-labeled calmodulin and EGFP-labelled protein kinase II (CaMKII) according to changes in intracellular calcium levels could be monitored [17, further publication in preparation]. While the calcium-calmodulin-dependent kinase was expressed intracellularly as a fusion protein to EGFP, synthetically labelled calmodulin was delivered via electroporation.

7 Summary and Outlook

Fluorescence correlation spectroscopy clearly approved of its future potential for biochemical research on both, in solution and in the living cell. Two initial intracellular dual-colour cross-correlation assays clearly demonstrated its capability to address reversible protein-protein interactions and ligand-binding in cells. Detailed intracellular mobility analysis of fusion-proteins were presented. Most of the reported studies were performed on home-built setups, including TPE with a pulsed laser system, but also with a commercial FCS setup (Zeiss ConfoCor II) featuring only one-photon excitation. Both modes of excitation succeeded in performing dual-colour FCS within cells, stimulating enhanced propagation of (dual-colour) FCS in general. Compared to FRET analysis in binding assays, FCS is not limited by steric requirements to its reporter molecules, whereas FRET appears to be the method of choice to study conformational changes. In contrast to optical methods relying on a pixel-by-pixel analysis of fluorescence images, FCS directly observes single diffusing reporter molecules and consequently allows for a simultaneous acquisition of multiple molecular parameters. Fluorescent proteins showed to be largely suitable for FCS: a) to be applied both in vitro and in vivo, b) for single colour as well as cross-correlation applications and c) for one-photon and two-photon excitation. During the next decade, fluorescent proteins will probably present the ultimate fluorescent probe for labelling proteins in vivo: they allow for highly precise and intracellular tagging, can be manipulated and optimised by genetic engineering and partly proved to act as biologically inert particles. Although smaller fluorescent tags would confer steric advantages no smaller candidate protein has been reported or indicated to our knowledge.

Acknowledgements We thank Elke Haustein for helpful discussion and proofreading the manuscript. Plasmids encoding the fluorescent proteins mRFP1 and tdimer2(12) were kindly provided by Roger Y. Tsien (University of California at San Diego).

References

1. Magde D, Elson EL, Webb WW (1972) Phys Rev Lett 29:705
2. Eigen M, Rigler R (1994) Proc Natl Acad Sci USA 91:5740
3. Schwille P, Meyeralmes FJ, Rigler R (1997) Biophys J 72:1878
4. Schwille P (2001) Cell Biochem Biophys 34:383
5. Denk W, Strickler JH, Webb WW (1990) Science 248:73
6. Schwille P, Haupts U, Maiti S, Webb WW (1999) Biophys J 77:2251
7. Heinze KG, Koltermann A, Schwille P (2000) Proc Natl Acad Sci USA 97:10377
8. Haupts U, Maiti S, Schwille P, Webb WW (1998) Proc Natl Acad Sci USA 95:13573
9. Schwille P, Kummer S, Heikal AA, Moerner WE, Webb WW (2000) Proc Natl Acad Sci USA 97:151
10. Heikal AA, Hess ST, Baird GS, Tsien RY, Webb WW (2000) Proc Natl Acad Sci USA 97:11996

11. Malvezzi-Campeggi F, Jahnz M, Heinze KG, Dittrich P, Schwille P (2001) Biophys J 81:1776
12. Miyawaki A (2002) Cell Struct Function 27:343
13. Zhang J, Campbell RE, Ting AY, Tsien RY (2002) Nature Rev Mol Cell Biol 3:906
14. Chen Y, Muller JD, Ruan QQ, Gratton E (2002) Biophys J 82:133
15. Ruan QQ, Chen Y, Gratton E, Glaser M, Mantulin WW (2002) Biophys J 83:3177
16. Bacia K, Majoul IV, Schwille P (2002) Biophys J 83:1184
17. Kim SA, Heinze KG, Waxham MN, Schwille P (2002) Biophys J (Annual Meeting Abstracts) 82:44a
18. Schwille P (2000) Cross-correlation analysis in FCS. In: Rigler R, Elson E (eds) Fluorescence correlation spectroscopy – theory and applications. Springer, Berlin Heidelberg New York, p 360
19. Krichevsky O, Bonnet G (2002) Rep Prog Phys 65:251
20. Haustein E, Schwille P (2002) Fluorescence correlation spectroscopy. Biophysics Online Textbook
21. Bacia K, Schwille P (2003) Methods (Duluth) 29:74
22. Rigler R, Mets U, Widengren J, Kask P (1993) Eur Biophys J 22:169
23. Widengren J, Mets U, Rigler R (1995) J Phys Chem 99:13368
24. Schwille P, Korlach J, Webb WW (1999) Cytometry 36:176
25. Wachsmuth M, Waldeck W, Langowski J (2000) J Mol Biol 298:677
26. Gennerich A, Schild D (2000) Biophys J 79:3294
27. Schwille P, Meyeralmes FJ, Rigler R (1997) Biophys J 72:1878
28. Ambrose WP, Goodwin PM, Jett JH, Van Orden A, Werner JH, Keller RA (1999) Chem Rev 99:2929
29. Dittrich P, Malvezzi-Campeggi F, Jahnz M, Schwille P (2001) Biol Chem 382:491
30. Eggeling C, Fries JR, Brand L, Günther R, Seidel CAM (1998) Proc Natl Acad Sci USA 95:1556
31. Nazarenko I, Pires R, Lowe B, Obaidy M, Rashtchian A (2002) Nucleic Acids Res 30: 2089
32. Harms GS, Cognet L, Lommerse PHM, Blab GA, Schmidt T (2001) Biophys J 80:2396
33. Labas YA, Gurskaya NG, Yanushevich YG, Fradkov AF, Lukyanov KA, Lukyanov SA, Matz MV (2002) PNAS 99:4256
34. Tsien RY (1998) Annu Rev Biochem 67:509
35. Palm GJ, Wlodawer A (GREEN FLUORESCENT PROTEIN 302 PG. 378–394. 1999 [Figures], [Plates], [Colour plates]
36. Nagai T, Ibata K, Park ES, Kubota M, Mikoshiba K, Atsushi M (2002) Nat Biotechnol 20:87
37. Griesbeck O, Baird GS, Campbell RE, Zacharias DA, Tsien RY (2001) J Biol Chem 276:29188
38. Matz MV, Fradkov AF, Labas YA, Savitsky AP, Zaraisky AG, Markelov ML, Lukyanov SA (1999) Nat Biotechnol 17:969
39. Baird GS, Zacharias DA, Tsien RY (2000) Proc Natl Acad Sci USA 97:11984
40. Sacchetti A, Subramaniam V, Jovin TM, Alberti S (2002) FEBS Lett 525:13
41. Yanushevich YG, Staroverov DB, Savitsky AP, Fradkov AF, Gurskaya NG, Bulina ME, Lukyanov KA, Lukyanov SA (2002) FEBS Lett 511:11
42. Campbell RE, Tour O, Palmer AE, Steinbach PA, Baird GS, Zacharias DA, Tsien RY (2002) Proc Natl Acad Sci USA 99:7877
43. Fradkov AF, Verkhusha VV, Staroverov DB, Bulina ME, Yanushevich YG, Martynov VI, Lukyanov S, Lukyanov KA (2002) Biochem J 368:17
44. Gross LA, Baird GS, Hoffman RC, Baldridge KK, Tsien RY (2000) Proc Natl Acad Sci USA 97:11990

45. Yarbrough D, Wachter RM, Kallio K, Matz MV, Remington SJ (2001) Proc Natl Acad Sci USA 98:462
46. Bevis BJ, Glick BS (2002) Nat Biotechnol 20:83
47. Terskikh A, Fradkov A, Ermakova G, Zaraisky A, Tan P, Kajava AV, Zhao X, Lukyanov S, Matz MV, Kim S, Weissman I, Siebert P (2000) Sci 290:1585
48. Erickson MG, Moon DL, Yue DT (2003) Biophys J 85:599
49. Gavin P, Devenish RJ, Prescott M (2002) Biochem Biophys Res Commun 298:707
50. Patterson GH, Lippincott-Schwartz J (2002) Science 297:1873
51. Ando R, Hama H, Yamamoto-Hino M, Mizuno H, Miyawaki A (2002) PNAS 99:12651
52. Zapata-Hommer O, Griesbeck O (2003) BMC Biotechnol 3:5
53. Karasawa S, Araki T, Yamamoto-Hino M, Miyawaki A (2003) J Biol Chem 278:34167
54. Griffin BA, Adams SR, Tsien RY (1998) Science 281:269
55. Adams SR, Campbell RE, Gross LA, Martin BR, Walkup GK, Yao Y, Llopis J, Tsien RY (2002) J Am Chem Soc 124:6063
56. Bae JH, Rubini M, Jung G, Wiegand G, Seifert MHJ, Azim MK, Kim JS, Zumbusch A, Holak TA, Moroder L, Huber R, Budisa N (2003) J Mol Biol 328:1071
57. Miyawaki A, Llopis J, Heim R, Mccaffery JM, Adams JA, Ikura M, Tsien RY (1997) Nature 388:882
58. Calleja V, Ameer-Beg SM, Vojnovic B, Woscholski R, Downward J, Larijani B (2003) Biochem J 372:33
59. Insall R (2003) Biochem J 372
60. Leaney JL, Benians A, Graves FM, Tinker A (2002) J Biol Chem 277:28803
61. Baird GS, Zacharias DA, Tsien RY (1999) Proc Natl Acad Sci USA 11241
62. Biondi RM, Baehler PJ, Reymond CD, Veron M (1998) Nucleic Acids Res 26:4946
63. Doi N, Yanagawa H (1999) FEBS Lett 453:305
64. Wyborski DL, Bauer JC, Vaillancourt P (2001) Biotechniques 31:618
65. Gossen M, Bujard H (1992) PNAS 89:5547
66. No D, Yao TP, Evans RM (1996) Proc Natl Acad Sci USA 93:3346
67. Piston DW, Patterson GH, Knobel SM (Methods in cell biology, vol 58: green fluorescent proteins 58 PG. 31-+. 1999 [Figures], [Plates], [Colour plates]
68. Tawa P, Tam J, Cassady R, Nicholson DW, Xanthoudakis S (2001) Cell Death Differentiation 8:30
69. Tramier M, Gautier I, Piolot T, Ravalet S, Kemnitz K, Coppey J, Durieux C, Mignotte V, Coppey-Moisan M (2002) Biophys J 83:3570
70. Weiss S (1999) Science 283:1676
71. Sako Y, Minoghchi S, Yanagida T (2000) Nature Cell Biol 2:168
72. Schutz GJ, Kada G, Pastushenko VP, Schindler H (2000) EMBO J 19:892
73. Dickson RM, Cubitt AB, Tsien RY, Moerner WE (1997) Nature 388:355
74. Garcia-Parajo MF, Segers-Nolten GMJ, Veerman JA, Greve J, van Hulst NF (2000) Proc Natl Acad Sci USA 97:7237
75. Llopis J, Mccaffery JM, Miyawaki A, Farquhar MG, Tsien RY (1998) Proc Natl Acad Sci USA 95:6803
76. Lodish H, Baltimore D, Berk A, Zipursky SL, Matsudaira P, Darnell J (1995) Molecular cell biology, 3rd edn. Scientific American Books, New York, p 640
77. Garcia-Parajo MF, Koopman M, van Dijk EMHP, Subramaniam V, van Hulst NF (2001) Proc Natl Acad Sci USA 98:14392
78. Wiedenmann J, Schenk A, Rocker C, Girod A, Spindler KD, Nienhaus GU (2002) PNAS 99:11646
79. Petersen J, Wilmann PG, Beddoe T, Oakley AJ, Devenish RJ, Prescott M, Rossjohn J (2003) J Biol Chem M307896200

80. Kask P, Palo K, Fay N, Brand L, Mets U, Ullmann D, Jungmann J, Pschorr J, Gall K (2000) Biophys J 78:1703
81. Chen Y, Muller JD, So PTC, Gratton E (1999) Biophys J 77:553
82. Palo K, Metz U, Jager S, Kask P, Gall K (2001) Biophys J 79:2858
83. Starchev K, Buffle J, Perez E (1999) J Colloid Interface Sci 213:479
84. Palmer AG, Thompson NL III (1987) Biophys J 52:257
85. Blab GA, Lommerse PHM, Cognet L, Harms GS, Schmidt T (2001) Chem Phys Lett 350:71
86. Denk W, Piston DW, Webb WW (1995) Two-photon molecular excitation in laser-scanning microscopy. In: Pawley JB (ed) Handbook of biological confocal microscopy. Plenum Press, New York, chap 28, p 445
87. Berland KM, So PTC, Gratton E (1995) Biophys J 68:694
88. Kohl T, Heinze KG, Kuhlemann R, Koltermann A, Schwille P (2002) PNAS 99:12161
89. Piston DW (1999) Trends Cell Biol 9:66
90. Cluzel P, Surette M, Leibler S (2000) Science 287:1652
91. Kohler RH, Schwille P, Webb WW, Hanson MR (2000) J Cell Sci 113:3921
92. Dittrich PS, Schwille P (2002) Anal Chem 74:4472
93. Schwille P, Oehlenschläger F, Walter NG (1996) Biochemistry 35:10182
94. Boukari H, Nossal R, Sackett DL (2003) Biochemistry 42:1292
95. Chen Y, Muller JD, Tetin SY, Tyner JD, Gratton E (2000) Biophys J 79:1074
96. Meseth U, Wohland T, Rigler R, Vogel H (1999) Biophys J 76:1619
97. Saito K, Ito E, Takakuwa Y, Tamura M, Kinjo M (2003) FEBS Lett 541:126
98. Verkman AS (2002) Trends Biochem Sci 27:27
99. Croce AC, Spano A, Locatelli D, Barni S, Sciola L, Bottiroli G (1999) Photochem Photobiol 69:364
100. Brock R, Hink MA, Jovin TM (1998) Biophys J 75:2547
101. Kettling U, Koltermann A, Schwille P, Eigen M (1998) Proc Natl Acad Sci USA 95:1416
102. Ha T, Enderle T, Ogletree DF, Chemla DS, Selvin PR, Weiss S (1996) Proc Natl Acad Sci USA 93:6264
103. Deniz AA, Laurence TA, Beligere GS, Dahan M, Martin AB, Chemla DS, Dawson PE, Schultz PG, Weiss S (2000) Proc Natl Acad Sci USA 97:5179
104. Selvin PR (2000) Nat Struct Biol 7:730
105. Oida T, Sako Y, Kusumi A (1993) Biophys J 64:676
106. Immink RGH, Gadella TWJ, Ferrario S, Busscher M, Angenent GC (2002) Proc Natl Acad Sci USA 99:2416
107. Patterson G, Day RN, Piston D (2001) J Cell Sci 114:837
108. Gurskaya NG, Fradkov AF, Terskikh A, Matz MV, Labas YA, Martynov VI, Yanushevich YG, Lukyanov KA, Lukyanov SA (2001) FEBS Lett 507:16